Eur. Phys. J. B **2**, 451–456 (1998)

THE EUROPEAN PHYSICAL JOURNAL B

Lattice damage and Al-metal precipitation in 2.5 MeV-electron-irradiated AlH_3

O.J. Zogal[1,a], P. Vajda[2,b], F. Beuneu[2], and A. Pietraszko[1]

[1] Institute of Low-Temperature and Structure Research, Polish Academy of Sciences, 50-950 Wroclaw 2, Poland
[2] Laboratoire des Solides Irradiés, CNRS-CEA, École Polytechnique, 91128 Palaiseau, France

Received: 20 October 1997 / Revised: 24 December 1997 / Accepted: 30 January 1998

Abstract. AlH_3 powder was bombarded with energetic electrons at 20 K and at room temperature and investigated by EPR, NMR, X-ray diffractometry, and microwave dielectric-constant measurements. The EPR spectra of the irradiated powder and of a selected single crystal cuboid of $\sim 10^{-1}$ mm edge show a complex asymmetric line centered at $g = 2.009$, with a Curie-like temperature dependence, attributed to radiation-induced color centers and/or their agglomerates. At the same time, the grains, which have become shiny black after irradiation, exhibit an increase of both the real and the imaginary part of ε. ^{27}Al-NMR spectra of the irradiated powder present a Knight-shifted line at 1600(50) ppm, close to the position of bulk metallic Al, and corresponding to a concentration of $c(\mathrm{Al}) \sim 10^{-2}$. In addition, the main hydride line differs from that before irradiation, demonstrating an alteration of environmental symmetry. The irradiation induces also a change in shape and width of the ^{1}H-NMR line, another indication of symmetry change in the lattice. Finally, a refined X-ray single-crystal structure analysis of the irradiated cuboid indicates a change of structure from trigonal $R{-}3c$ to $R{-}3$, with a loss of mirror symmetry for the two Al sites caused by the introduction of Al-defects in the vicinity of one of them.

PACS. 61.72.Ji Point defects (vacancies, interstitials, color centers, etc.) and defect clusters – 76.30.Mi Color centers and other defects – 76.60.Cq Chemical and Knight shifts

1 Introduction

Aluminium trihydride has been considered for some time as a potentially interesting hydrogen storage material, in view of the low price of the matrix metal and the high concentration of the hydrogen present, but the difficulties of its preparation have prevented a broad technical application [1]. Even then, the practically unlimited stability of AlH_3 at room temperature together with the facile decomposition above 100 °C are the reason for continued investigation of its physical and physico-chemical properties under various environmental conditions. From a fundamental point of view, it seems important to characterize intrinsic lattice defects such as colour centers and to study their eventual transformation to larger agglomerates and colloids in this material.

The crystal structure of AlH_3 has been determined through powder diffractometry by Turley and Rinn [2] as belonging to the trigonal space group $R{-}3c$ (D^6_{3d}), with six AlH_3 molecules per hexagonal unit cell. A calorimetric study of the thermodynamic properties of AlH_3 was performed by Sinke *et al.* [3] and the equilibration kinetics of its decomposition at 140 and 150 °C in gaseous atmosphere was determined by Baranowski and Tkacz [4]. Zogal *et al.* [5,6] had undertaken ^{1}H and ^{27}Al nuclear magnetic resonance (NMR) experiments on AlH_3 powder in the range 4.3−300 K and observed complex proton spectra at higher temperatures, attributed to the presence of molecular surface hydrogen; no Al Knight shift had been noted. Kinetic and microscopic studies of the thermal and photolytic decomposition products were done by Herley *et al.* [7] who watched acicular Al filaments agglomerate together into thicker lumps; observation of pristine AlH_3 under the beam of a 100 keV electron microscope led by itself, within seconds, to brutal decomposition into an Al residue [8]. Finally, it was shown [9] that u.v. radiation induced at 77 K colour centers giving rise to an electron-spin-resonance (ESR) signal at $g = 1.995$ which disappeared upon heating to room temperature.

In the present work, we have created lattice damage in AlH_3 powder by irradiating with energetic electrons in a van de Graaff accelerator, with a very low particle fluence compared to the beam of an electron microscope. We have studied this damage by measuring the ESR, NMR, X-ray diffraction, and microwave dielectric constant, ε, and note, in addition to colour centers, the presence of metallic Al

[a] e-mail: zogal@int.pan.wroc.pl
[b] e-mail: peter.vajda@polytechnique.fr

colloids and, probably related, a crystal lattice transformation from $R{-}3c$ to $R{-}3$ (D^6_{3d} to C^2_{3i}).

2 Experimental

The investigated specimens were AlH_3 powder as used in previous work [5,6] and stored in dry air. They consisted of cuboids of roughly 100 μm edge length. Most of them were twins, but a few – selected under the microscope – were good quality single crystals, and could be used for X-ray crystallography.

For damage introduction, 20−25 mg AlH_3 powder were sealed in 20 μm thick copper foil attached to a holder and irradiated with 2.5 MeV electrons of the van de Graaff accelerator at Palaiseau in a liquid hydrogen cryostat. To make sure that no excessive heating by the electron beam was inducing thermal decomposition, we have undertaken two irradiations: one at 21 K, the other at 280 K, the temperature being checked by a thermocouple soldered to the copper bag. Typical beam currents of 30 μA/cm^2 were used to give integrated doses of 2 to 3 C/cm^2. No influence of the irradiation temperature was noted. Since the range of 2.5 MeV electrons in Al is of the order of 5 mm [10], the damage distribution in the powder was sufficiently uniform throughout its thickness, which did not exceed 1 mm. After irradiation, the sample holder was removed at room temperature from the accelerator and the powder transferred to the various measuring setups.

X-band (f = 9.4 GHz) ESR experiments were performed on a Bruker ER 200 D spectrometer (nominal Klystron power 250 mW) equipped with a one-axis goniometer and with an Oxford Instruments liquid-helium cryostat in the 4−300 K range. The measurements were done either on the powder, filled into a high-purity quartz tube with helium gaz, or on a single crystal cuboid fixed with a signal-free grease on a quartz rod such that its face normal could be rotated with respect to the static magnetic field orientation.

Room-temperature dielectric-constant measurements were done on the powder using the same quartz tube as for ESR introduced into a small hole drilled in a TE_{10n} rectangular cavity. Eight resonant modes of the cavity with an electric-field maximum at the sample site were observed in the range 7−15 GHz with a Hewlett-Packard 8510 C network analyzer. The width and frequency variations of the resonance curves taken with and without the sample permitted to calculate, for each mode, the real (ε') and the imaginary (ε'') components of the dielectric constant, $\varepsilon = \varepsilon' - i\varepsilon''$.

The NMR measurements were made at 7.05 T on a Bruker MSL 300S spectrometer equipped with a fast digitalizer allowing for spectral windows of up to 2.5 MHz. The resonance data were obtained at nominal frequencies 78.206 MHz and 300.13 MHz for the ^{27}Al and ^{1}H nuclei, respectively. A high-power probehead with a 5 mm diameter solenoid coil was used. Two equal-width-pulse solid-echo sequences or single-pulse excitations were applied to obtain the ^{27}Al signal. The spectra are Fourier transforms from the resulting echo and free induction decays. The proton spectra were taken after Fourier transformation of an half echo in $90{-}\tau{-}180{-}\tau{-}$echo pulse sequence, with a pulse separation τ of 7 μs. The temperature was varied from 20 to 292 K (for ^{27}Al NMR) using a temperature controller ITC-4 from Oxford Instruments.

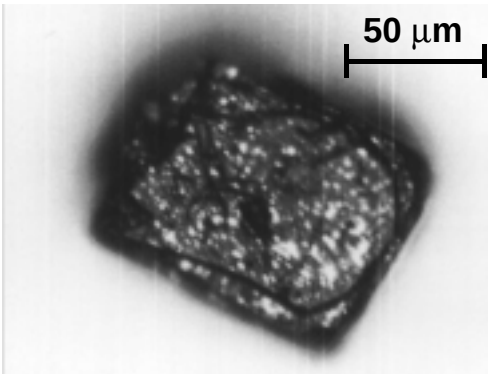

Fig. 1. Optical micrograph of a single cuboid grain of AlH_3, exhibiting elliptical metallic Al flakes of $\leq$ 1 μm in length after irradiation at 21 K with 2.5 MeV electrons to a dose of 3 C/cm^2.

X-ray crystallography was carried out at room temperature on single-crystals cuboids using the full automatic KUMA-Diffraction KM4 four-circles diffractometer (Ω/Θ scan), employing graphite-monochromated Mo Kα_1 radiation (λ = 0.71073 Å). The sample examination (determination of the spread-angle mosaicity and of the shape of the reflections) was performed using the MK4CCD diffractometer with a two-dimensional CCD detector. Empirical absorption corrections were applied basing on a Ψ-scan for selected reflections. The reflected intensities were corrected for the Lorentz and polarization effects. The crystal structure was solved using the Patterson method and a refined full-matrix least-squares fit.

3 Results and discussion

Under irradiation with electrons, the originally dull grey powder turns shiny black and the cuboid grains exhibit under the microscope a surface covered with brilliant metallic-like flakes of elliptic shape, typically 1 μm in length (Fig. 1). This reminds us of the description [7] of the thermal decomposition of AlH_3 at 140 °C, resulting in acicular Al filaments clustering together to form small clumps. As already mentioned in the preceding section, we can exclude a thermal decomposition process in our case, since both irradiations, at 21 K and at room temperature, had identical effects. In the following, we shall present and discuss the relevant results of various physical measurements.

3.1 Dielectric constant

The microwave dielectric constant measured at room temperature on the AlH_3 powder had clearly increased

after irradiation. Thus, typical values, for the pristine material, obtained at a mean frequency of $f = 10$ GHz, were $\varepsilon' = 4.25(10)$ and $\varepsilon'' = 0.029(3)$; they changed to $\varepsilon'_{irr} = 5.30(10)$ and $\varepsilon''_{irr} = 0.089(5)$ upon irradiation, a significant increase, in particular as concerns the imaginary part, which is related to the microwave conductivity, $\sigma = \varepsilon_0 \varepsilon'' \omega$.

One can try to describe the present situation in a classical two-component model treating the sample as a mixture of dielectric spheres embedded in an insulating matrix (Maxwell Garnett model, see *e.g.* Ref. [11]). For the case of metallic inclusions, with $\varepsilon''_m \gg 1$, and for small concentrations $x \ll 1$ (which is the case in this experiment), it can be shown that

$$\varepsilon' = \varepsilon_h(1 + 3x) \text{ and } \varepsilon'' = (\varepsilon_h^2/\varepsilon''_m)9x$$

(ε_h is the relative dielectric constant of the host matrix; ε''_m for 10 GHz becomes, with $\sigma(\mathrm{Al}) = 3.5 \times 10^7\ \Omega^{-1}\mathrm{m}^{-1}$, $\varepsilon''_m = 6.3 \times 10^7$). It is evident that increases $\Delta\varepsilon'_{irr}$ and $\Delta\varepsilon''_{irr}$ such as measured after irradiation cannot be accounted for in this simple isotropic model. On the other hand, a generalization to non-spherical inclusions, with a depolarizing factor n (for spheres, $n = 1/3$) leads to the expressions:

$$\varepsilon' = \varepsilon_h(1 + x/n) \text{ and } \varepsilon'' = (\varepsilon_h^2/\varepsilon''_m)x/n^2.$$

Flat or needle-shaped inclusions, possessing small n-values, could give substantial ε-increases. This is encouraging, in view of the microscopic observations described above.

It might be interesting, in this context, to recall the quasi inverse experiment to ours: the introduction of solute hydrogen into aluminium by chemical and electrochemical charging [12]. There, the authors had observed that the vacancies introduced simultaneously with the hydrogen clustered to form platelet-like defects.

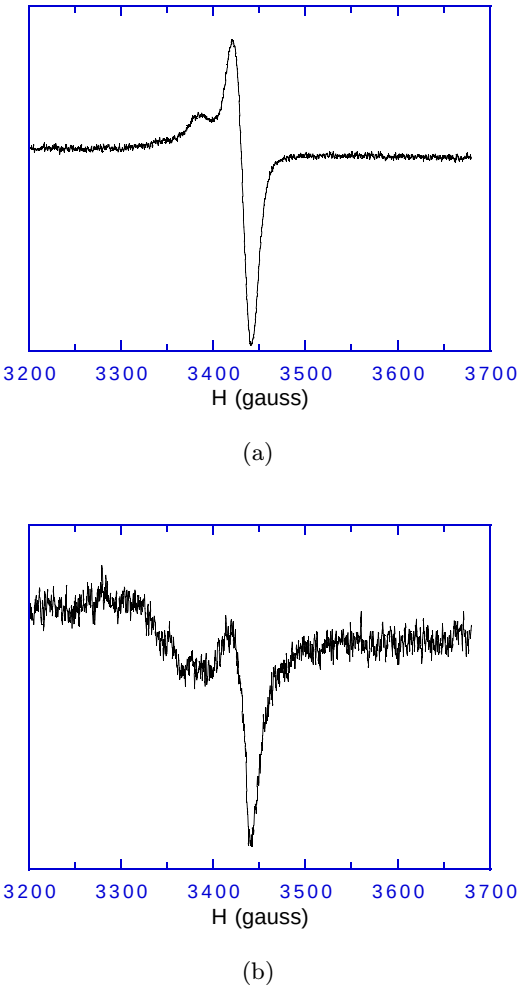

Fig. 2. (a) ESR spectrum (at 300 K) of 20.5 mg AlH_3 powder irradiated at 280 K with 2.5 MeV electrons to a dose of 2 C/cm^2. Attenuation $P = 14$ dB (corresponding to 10 mW microwave power), modulation $M = 0.2$ mT; (b) ESR spectrum (at 4 K) of a single-crystal cuboid of AlH_3 (1.5 μg), with one edge oriented parallel to H_0. $P = 20$ dB (2.5 mW), $M = 1$ mT.

3.2 Electron spin resonance

After what was described above, it seemed natural to look for a signal of metallic aluminium by conduction ESR. The signal-free ESR spectrum of the unirradiated powder had changed, after electron bombardment, exhibiting the lines shown in Figure 2. Both, the upper spectrum, taken with the whole (20.5 mg) amount of powder, and the lower spectrum, taken on a single (1.5 μg) grain, possess a qualitatively similar aspect. The signal consists of a very asymmetric line centered at $g = 2.009(1)$ of $\Delta H = 2$ mT width, accompanied by a shoulder near $g = 2.040$. This line behaves Curie-like with temperature, which permits to record the signal of the single grain ($< 10^{-4}$ of the powder mass) by taking it at 4 K. The signal is isotropic; rotation of the cuboid with respect to its axis did not change the position nor the shape of the line.

The temperature dependence of the line intensity as well as its position disaffirm its assignation to metallic Al. (The g-value of Al metal was determined to $g = 1.997(1)$ by Schultz *et al.* [13].) On the other hand, the lack of anisotropy does not favour colour centers from simple point defects. We are, therefore, inclined to attribute the line at $g = 2.009$ to small but already close to spherical defect aggregates, maybe aggregates of H-vacancies serving as precursors to metallic Al colloids. In any case, our signal is not identical with that observed in reference [9] at $g = 1.995$ in u.v.-illuminated AlH_3 – which was much narrower ($\Delta H = 0.25$ mT) and only stable at low temperatures – and attributed to colour centers playing a role in the photolytic decomposition process.

One might wonder about the non-observation of a signal due to metallic Al in our measured ESR spectra after irradiation, in view of the other signs for its presence already described above and also to be shown below. This is probably related to the very unfavourable conditions for the observation of a CESR signal. In fact,

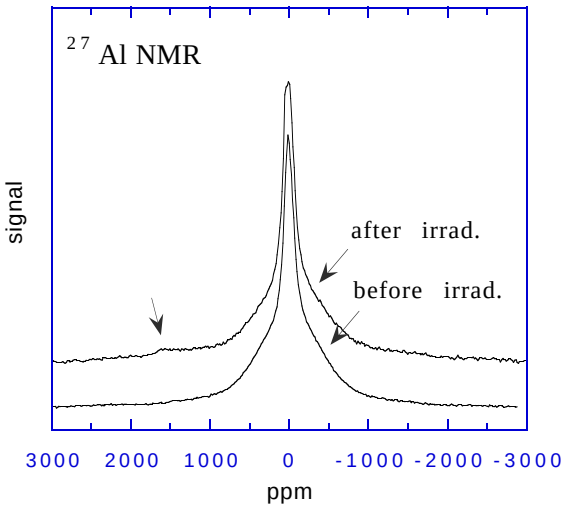

Fig. 3. Room-temperature ^{27}Al NMR spectra of electron-irradiated (above, see irradiation conditions of Fig. 2a) and non-irradiated (below) AlH_3 powder. Note the broadening of the central line and the appearance of a signal near 1600 ppm due to metallic Al, after irradiation.

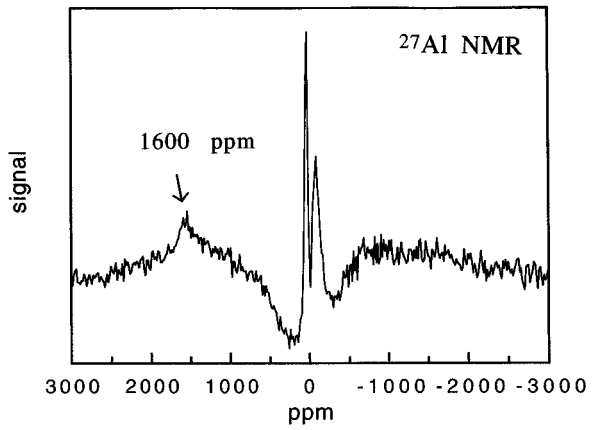

Fig. 4. Difference plot of the two ^{27}Al NMR spectra of Figure 3, indicating the Knight-shifted signal and the change in the central line shape.

the temperature dependence of its linewidth [13] would require an investigation at T below 30 K, where its Pauli-type (T-independent) susceptibility would become completely masked by the growth of the Curie-type signal at $g = 2.009$.

3.3 Nuclear magnetic resonance

3.3.1 ^{27}Al NMR

Under our experimental conditions, the lineshape in the pristine sample is symmetrical and consists of a powder pattern typical of a first-order quadrupolar interaction (Fig. 3). The main spectral feature is the large line (central $+1/2 \leftrightarrow -1/2$ transition) situated around 0 ppm relatively to an $AlCl_3$ aqueous solution. The accompanying satellite transitions $\pm 3/2 \leftrightarrow \pm 1/2$ and $\pm 5/2 \leftrightarrow \pm 3/2$ are clearly seen but remain unsplit and possess much smaller intensity. This observation is in accord with the earlier investigation [5].

The ^{27}Al spectrum of the irradiated sample exhibits some resemblance to the non-irradiated one but also some dissimilarity. A new feature (resonance line) is seen at about 1600 ppm above the frequency of the most intense $+1/2 \leftrightarrow -1/2$ transition of AlH_3. Within experimental accuracy (±30 ppm), the position of the line does not show any clear temperature dependence in the measured range, 20 to 300 K. These characteristics are very close to those of the signal of ^{27}Al NMR in metallic aluminium, where a Knight shift of 1640 ppm and only a weak temperature dependence were observed, according to the review by Carter *et al.* [14]. The comparison of these data with the noted ones in our specimen suggests strongly that the observed resonance originates from the metallic aluminium formed during the irradiation process. Its relative intensity was determined to an order of magnitude by integration of the whole spectrum on a large piece of strong paper and weighing the corresponding parts; the main error coming from a possible overlap of the main line, we estimate the Al-concentration to less than 1 at.%.

Although the main ^{27}Al resonance bears similar hallmarks for both the irradiated and the non-irradiated sample, small but apparently significant differences should be mentioned and are presented, together with the Al-metal signal, in the difference plot of Figure 4. The central transition of the irradiated sample is somewhat broader and can be decomposed as the superimposition of two slightly shifted lines of the same intensity. Also the satellites seem more accentuated. A ^{27}Al magic-angle-spinning (MAS) experiment would be useful to get a deeper insight for the understanding of this part of the spectrum, by narrowing and hence eventually separating overlapping signals. On the other hand, X-ray crystallographic data (see below) indicate that, in the irradiated AlH_3 structure, there are two non-equivalent Al atoms with the same occupation number. It seems, therefore, quite reasonable to assume that the new feature stems from the crystal structure difference between irradiated and non-irradiated material.

3.3.2 ^{1}H-NMR

The observed proton NMR absorption spectra display a superimposition of two resonance lines with different widths and intensities (Fig. 5). Such specific character of the spectra was already reported in reference [5] for a pristine AlH_3 sample, where CW NMR and a magnetic field of 0.35 T had been used.

The resonance lineshape of the irradiated sample is close to Gaussian while the signal of the non-irradiated one is rather triangular. Though it is difficult to separate the two components in an unambiguous way, we have estimated the full widths at half maximum (FWHM) of the broad lines to 83 kHz and to 64 kHz for the irradiated and the non-irradiated specimens, respectively. The line broadening after irradiation can be understood in terms of new

Table 1. Atomic coordinates, occupancy factors (PP), multiplicities (m), Wyckoff positions (W), and site symmetries (s).

	x	y	z	PP	m	W	s
Al_1	0.000	0.000	0.000	0.978	3	a	-3
Al_2	0.000	0.000	0.500	1.000	3	b	-3
Al_3	0.000	0.000	0.6678(20)	0.022	6	c	3
H_1	0.3445(41)	0.2940(44)	0.4197(16)	1.000	18	f	1

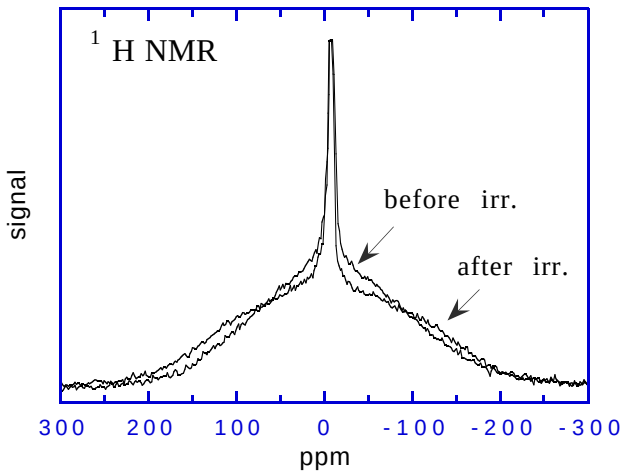

Fig. 5. ^{1}H NMR spectra of irradiated and non-irradiated AlH_3 powder (same as employed for ^{27}Al NMR in Fig. 3). Note the shape change of the broad component of the resonance line due to introduced defect centers during irradiation.

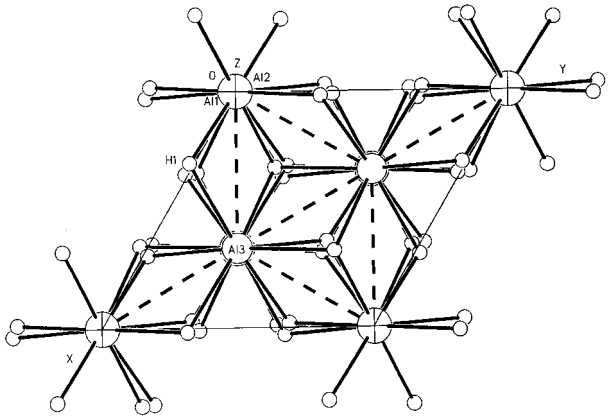

Fig. 6. (001) projection of the hexagonal unit cell of the irradiated AlH_3-structure in the space group $R-3$ (identical, in this view, to $R-3c$ of the pristine material).

paramagnetic centers created in the irradiation process, which are coupling to the protons by direct dipole-dipole interaction. An additional broadening mechanism is due to the demagnetizing field in our powder specimen, which is an especially efficient mechanism when the NMR experiments are performed at high fields, such as in the present case (7.05 T).

3.4 X-ray crystallography

We had succeeded in isolating single grains ($\sim$ 100 μm size) of the AlH_3 powder which were twin-free and of sufficient quality to allow us to perform single-crystal structure analysis. The investigated crystals exhibited a very large spread-angle mosaicity as observed with a two-dimensional CCD detector. The data were obtained with Mo Kα_1 radiation ($\lambda = 0.71073$ Å) and treated using 357 independent reflections out of a total of 1477 collected reflections, in the index ranges $-8 \le h \le 8$, $-8 \le k \le 8$, $-23 \le l \le 23$, spanning the interval $11° \le 2\Theta \le 90°$.

It had been found from powder diffractometry [2] that the symmetry of the crystal structure could be described by the $R-3c$ (D^6_{3d}) space group. Our single-crystal experiment indicated that the space groups $R-3$ (C^2_{3i}), $R-3m$ (D^5_{3d}), $R3m$ (C^5_{3v}), $R32$ (D^7_3), and $R3$ (C^4_3) were possible. After refinement of the crystal structures for all space groups, using a full-matrix least-squares fit, the $R-3$ space group was selected having a discrepancy factor $R = 0.0386$. (The lowest value for the discrepancy factor, $R = 0.026$, was obtained for $R-3$m symmetry, but the crystal structure was disordered. In fact, the H-atoms occupied statistically two positions around the mirror plane and the Al_1 atom was smeared out upon six equivalent positions.) The new lattice parameters are $a = 4.451(1)$ Å and $c = 11.766(2)$ Å as compared to the 4.449 Å and 11.804 Å, respectively, of the original material [2], with a corresponding density increase from $d = 1.477(1)$ to 1.481(1) g/cm^3, after irradiation.

The crystal structure is shown in Figures 6 and 7 in a (001) projection and a (010) view of the hexagonal unit cell, respectively. The atomic coordinates are shown in Table 1. The principal modification when going from $R-3c$ to $R-3$ symmetry is the loss of the glide mirror plane c and the fact that the Al atoms occupy the two Wyckoff positions (3a and 3b, for $R-3$). In addition, new sites have been found from the difference maps, which could possibly be occupied by Al-atoms (designated as Al_3 in Figs. 6 and 7). As seen in Figure 7, the two sites indicated as Al_1 and Al_2 have now a different environment caused by the presence of Al_3. At the same time, this distortion results in a change of various intracell distances. Thus, in particular the atom Al_2, having in its neighbourhood two atoms Al_3 at a distance of 1.984 Å, is found with a bridging distance Al_2-H_1 of 1.754 Å, while the undisturbed Al_1-H_1 remains 1.718 Å as in the pristine $R-3c$ [2]; the coordination

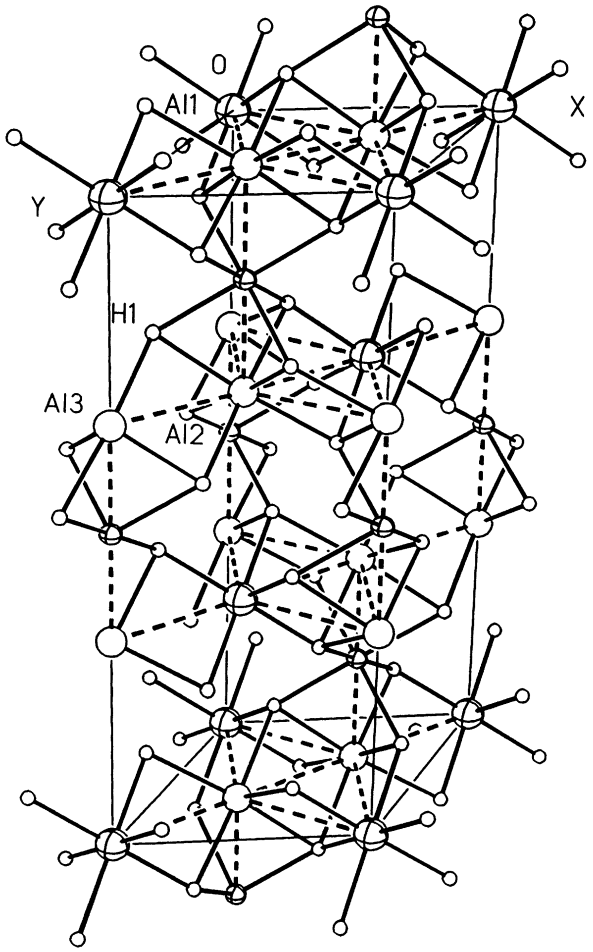

Fig. 7. Irradiated AlH_3-structure in the space group $R{-}3$ viewed along the (010) axis of the hexagonal unit cell, indicating the non-equivalent sites Al_1 and Al_2, due to the introduced defects Al_3 (see text).

Table 2. Interatomic bond lengths (Å) in irradiated AlH_3.

Al_1-H_1	1.72(2)	Al_1-Al_3	2.5699(6)
Al_2-H_1	1.75(2)	Al_2-Al_3	1.98(2)
Al_3-H_1 [(a)]	1.80(2)		
Al_3-H_1 [(b)]	1.88(2)		

(a) corresponding to the symmetry transformation: $-z + 1/3$.
(b) corresponding to the symmetry transformation: $z - 1/3$.

of the Al_3 atoms is octahedral, with two Al_3-H_1 distances equal to 1.80 and 1.88 Å (Tab. 2).

As to the character of the Al_3 atoms, their concentration of $\sim$ 2 at%, the localisation of their lattice sites on the Al c-axis, and the slightly repulsive action resulting in an increasing a, speaks in favour of their attribution to the Al we have observed and described in the preceding subsections.

4 Conclusions

High-energy low-flux electron irradiation induces in AlH_3 powder lattice defects (colour centers or their clusters) detected by EPR (signal at $g = 2.009$), ^{1}H NMR and ^{27}Al NMR (change in line shape). In addition, anisotropic metallic Al-precipitates are manifest through an Al-Knight shift in ^{27}Al NMR and an increase in the dielectric constant. The introduced damage is accompanied by a structure change from $R{-}3c$ to $R{-}3$ (loss of mirror symmetry between the two base Al atoms) as found through single-crystal X-ray structure analysis.

References

1. R. Wiswall, chapter 5 in *Hydrogen in Metals. II,* edited by G. Alefeld, J. Vöslkl (Springer, Berlin, 1978) p. 201.
2. J.W. Turley, H.W. Rinn, Inorg. Chem. **8**, 18 (1969).
3. G.C. Sinke, L.C. Walker, F.L. Oetting, D.R. Stull, J. Chem. Phys. **47**, 2759 (1967).
4. B. Baranowski, M. Tkacz, Z. Phys. Chem. NF **135**, 27 (1983).
5. O.J. Zogal, B. Stalinski, S. Idziak, Z. Phys. Chem. NF **145**, 167 (1985).
6. O.J. Zogal, M. Punkkinen, E.E. Ylinen, B. Stalinski, J. Phys. Cond. Matter **2**, 1941 (1990).
7. P.J. Herley, O. Christofferson, J.A. Todd, J. Solid State Chem. **35**, 391 (1980); P.J. Herley, O. Christofferson, R.H. Irwin, J. Phys. Chem. Solids **85**, 1874 (1981); P.J. Herley, O. Christofferson, *ibid.* **85**, 1882 (1981).
8. P.J. Herley, W. Jones, J. Mat. Sci. Lett. **1**, 163 (1982).
9. A.P. Bobrovskii, Yu.D. Pimenov, Opt. Spektrosc. **39**, 565 (1975).
10. L. Pagès, E. Bertel, H. Joffre, L. Sklavenitis, Commissariat à l'Énergie Atomique Report CEA-R-3942 (1970).
11. R. Landauer, in *AIP Conf. Proceedings* N° 40 (N.Y., 1987) p. 2.
12. H.K. Birnbaum, C. Buckley, F. Zeides, E. Sirois, P. Rozenak, S. Spooner, J.S. Lin, J. Alloys Compounds **253-254**, 260 (1997).
13. S. Schultz, G. Dunifer, C. Latham, Phys. Lett. **23**, 192 (1966).
14. G.C. Carter, L.H. Bennett, D.J. Kahan, *Metallic Shifts in NMR*, Progress in Materials Science, edited by B. Chalmers *et al.*, vol. 20 (Pergamon Press Oxford, 1997).